Supporting Information

Gao et al. 10.1073/pnas.1625010114

SI Text

Raman Characterization of Graphene Before and After Modification. Raman spectroscopy is widely used to characterize the quality and doping level of graphene films (30). In this work, Raman spectra were obtained from graphene sheets before/after pyrene butyric acid (PYCOOH) and polyethylene glycol (PEG) modification steps (see detailed modification procedures in *Materials and Methods*) in air (Fig. S2). A typical Raman spectrum of bare graphene transferred to a SiO_2/Si substrate used for device fabrication (Fig. S2*A*) shows features representative of a high-quality graphene monolayer, including negligible D peak at ∼1,350 cm^{-1}, narrow 2D peak at ∼2,680 cm^{-1} (FWHM = 43 cm^{-1}) and a 2D-to-G intensity ratio, I_{2D}/I_G, of >2. Quantifying the I_{2D}/I_G ratio from 2D maps of representative 10 × 10-μm^2 areas yields an average ±1 SD of 3.6 ± 0.5, which is consistent with monolayer graphene (30).

In addition, 2D maps of the graphene G-band shift measured from 10 × 10-μm^2 graphene regions before and after PYCOOH and PEG modification steps (Fig. S2*B*), yield a significant downshift in the average values from 1,594 to 1,591 and then to 1,585 cm^{-1}, respectively. Previous work has shown that the Raman G peak, which corresponds to the E_{2g} phonon at the Brillouin zone center, will stiffen with p-type and soften with n-type doping, leading to upshifts or downshifts in Raman spectra (44). Pristine undoped monolayer graphene shows a G band at 1,584 cm^{-1}, whereas the G band of the bare graphene measured in our experiment, 1,592 cm^{-1}, indicates a substrate-induced p-doping effect (45). Both PYCOOH and PEG modifications lead to electron or n-type doping, resulting in the observed downshift of the G band. In comparison, the CNP measurements (Fig. 2*C*), which were carried out in pH 7.4 1× PBS, show the same overall effect from bare to PEG-modified graphene devices with a 0.55 ± 0.08 to 0.22 ± 0.06 V shift that is consistent with n-type doping (33). The initial modification step with PYCOOH does not show a statistically significant CNP change, 0.55 ± 0.08 to 0.62 ± 0.07 (Fig. 2*C*), although this difference compared with dry-state Raman can be attributed to deprotonation of the PYCOOH carboxylic acid group in 1× PBS used for the electrical measurements.

Estimate of PEG Layer Dielectric Constant. The PEG modification layer adds a hydrated dielectric polymer layer on graphene, and thus the overall interfacial capacitance of the PEG modified graphene devices is composed of graphene quantum capacitance (C_q) and PEG-induced capacitance (C_{PEG}) in series (46), shown as Eq. **S1**:

$$\frac{1}{C_{overall}} = \frac{1}{C_q} + \frac{1}{C_{PEG}}. \quad \textbf{[S1]}$$

C_q for bare graphene, ∼7 $\mu F/cm^2$, and the overall interfacial capacitance in 100 mM NaCl (pH 7) solution, ∼5 $\mu F/cm^2$, have been reported previously (46). Because the interfacial capacitance is proportional to the transconductance of FET devices (47), the values measured in Fig. 3*D* for bare and PEG-modified graphene yield an estimated C_{PEG} of ∼4.2 $\mu F/cm^2$. Given the thickness of PEG measured by AFM (Fig. 2*A*), ∼6 nm, the dielectric constant of PEG layer, $\varepsilon_{r,PEG}$, estimated using Eq. **S2**,

$$C_{PEG} = \frac{\varepsilon_{r,PEG}\varepsilon_0}{d_{PEG}}, \quad \textbf{[S2]}$$

is 28, where C_{PEG} is the capacitance of the PEG layer, ε_0 is the electric constant, and d_{PEG} is the PEG layer thickness. Reported measurements of the dielectric constant of PEG in aqueous solution show a monotonic decrease with increasing PEG concentration, and thus our estimated value lies between dehydrated PEG, 11.8, and water, ∼80 (48). Our analysis suggests that the PEG layer on the graphene devices is partially hydrated in buffer solution and consistent with our hypothesis, although future work will be needed to fully characterize the properties of the PEG layers.

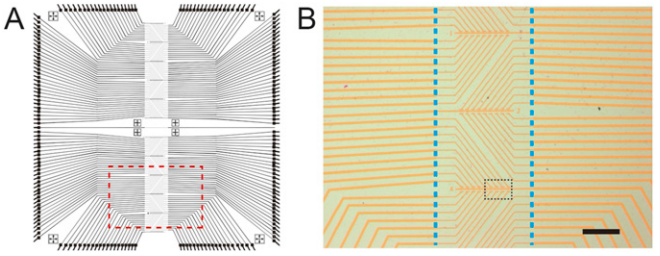

Fig. S1. Sensor chip device layout. (*A*) Overall layout of the sensor chip consisting of 180 individually addressable graphene transistors. The thicker outer lines correspond to gold metal interconnects, which terminate at wire-bonding pads at the chip periphery, and the thinner lines in the central vertical region correspond to the source and drain connections. Image size: 10 × 10 mm^2. (*B*) Optical image of graphene devices from the region highlighted by red-dashed box in *A*. The yellow–orange lines correspond to the gold metal source and drain electrodes that connect individual graphene devices. The position of the microfluidic channel used to deliver samples is highlighted by the two vertical dashed blue lines. (Scale bar: 100 μm.) The black dashed box highlights the region corresponding to Fig. 1*C*.

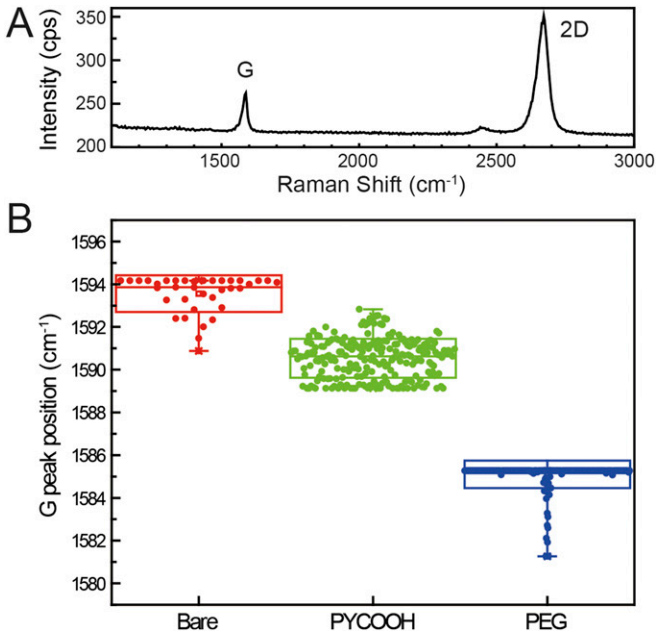

Fig. S2. Raman characterization of graphene before and after surface modification steps. (*A*) Raman spectrum of bare graphene, where the graphene was transferred to a SiO_2/Si substrate. The G and 2D bands (*SI Text*) are highlighted. (*B*) Box plots of Raman G peak shift before and after PYCOOH and PEG modifications measured from a 10 × 10-μm^2 graphene region. The highest and lowest horizontal lines in the boxes represent SD, whereas the middle line represents the mean value. The vertical lines highlight the maximum and minimum values. The average G peaks of pristine graphene (red), PYCOOH-modified graphene (green), and PEG-modified graphene (blue) are located at 1,594, 1,591, and 1,585 cm^{-1}, respectively. The downshift of the G band indicates electron doping due to the PYCOOH and then PEG modification steps. Raman spectra were acquired with a LabRam Evolution Multiline Raman Spectrometer (Horiba) equipped with 600 blaze/mm grating and a 100× microscope objective lens (numerical aperture of 0.95) and 532-nm wavelength continuous-wave diode laser.

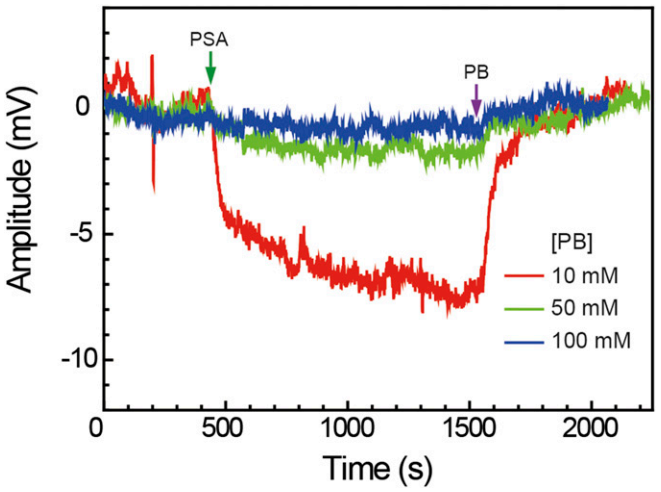

Fig. S3. Nonspecific protein detection on graphene sensors. Response of an ethanolamine (ETA)-modified graphene sensor vs. time during addition of 100 nM prostate-specific antigen (PSA) in pH6 phosphate buffer (PB) (green arrow) and subsequent addition of pure PB (purple arrow). The red, green, and blue traces correspond to PB concentrations of 10, 50, and 100 mM, respectively. The signal amplitudes were 7.5, 1.5, and 0.4 mV for 10 mM (red), 50 mM (green), and 100 mM (blue) PB conditions, respectively. The 50 mM trace is also shown in Fig. 3*A* as a control. ETA was coupled to PYCOOH-modified graphene surface (see *Materials and Methods* for detailed procedures) to yield a hydroxyl-terminated graphene surface. The ETA-modified sensors show a much smaller PSA response vs. PB concentration compared with PEG/ETA-modified sensors, consistent with the concept that the permeable PEG layer increases the effective Debye screening length.